*applied mechanics*

*Article*

# Analysis of Acid Diffusion Effects on Physical Properties of Polymer Composites: A Combined Study of Mechanical and Electrical Characterization

**Sebastian Tamayo-Vegas [1,*], Khalid Lafdi [1,2], Mostapha Tarfaoui [3], Khalil K. Lafdi [4] and Mohamed Daly [3]**

1 Department of Mechanical Engineering, Northumbria University, Newcastle upon Tyne NE1 8ST, UK; khalid.lafdi@northumbria.ac.uk
2 Department of Chemical Engineering, University of Dayton, Dayton, OH 45469, USA
3 ENSTA Bretagne, IRDL UMR CNRS 6027, F-29200 Brest, France; mostapha.tarfaoui@ensta-bretagne.fr (M.T.); mohamed.daly@ensta-bretagne.fr (M.D.)
4 Gosforth Academy, Gosforth, Newcastle upon Tyne NE3 2JH, UK; khalilboeing@gmail.com
* Correspondence: w18002002@northumbria.ac.uk

**Abstract:** In this study, we examined the impact of carbon nanotube (CNT) concentration on the mechanical properties of epoxy/CNT composites under acid exposure. Samples with varying CNT concentrations (0% to 5%) were fabricated and characterized using dynamic mechanical analysis (DMA) and nanoindentation. Beyond the percolation threshold, the composites experienced decreased bulk mechanical properties due to CNT agglomeration. Acid exposure for one week and one month revealed a gradient of properties from the sample's skin to its core. Overall, the composites exhibited modified physical properties, with degradation influenced by the CNT concentration. Higher concentrations acted as barriers but also created pathways for acid diffusion through pores surrounding CNT agglomerates. The agreement between nanoindentation and vector network analyzer (VNA) measurements further supported our findings. This convergence of mechanical and electromagnetic characterization techniques holds promise for wireless structural health monitoring (SHM) applications. Our study enhances the understanding of epoxy/CNT composites for SHM applications. The relationship between CNT concentration, acid exposure, and mechanical properties guides material selection and the development of real-time damage-detection techniques. Integrating multiple measurement techniques, as demonstrated by the agreement between nanoindentation and VNA data, provides a comprehensive understanding of structural behavior, improving SHM practices.

**Keywords:** polymer composites; nanoindentation; vector network analyzer; acid diffusion; structural health monitoring



**Citation:** Tamayo-Vegas, S.; Lafdi, K.; Tarfaoui, M.; Lafdi, K.K.; Daly, M. Analysis of Acid Diffusion Effects on Physical Properties of Polymer Composites: A Combined Study of Mechanical and Electrical Characterization. *Appl. Mech.* **2023**, *4*, 974–989. https://doi.org/10.3390/applmech4030050

Received: 30 June 2023
Revised: 10 August 2023
Accepted: 26 August 2023
Published: 31 August 2023



## 1. Introduction

Polymer nanocomposite materials are widely used across various industries [1–4]. Many of these structures and parts function in harsh environments and working conditions. Furthermore, several composites are exposed to aggressive chemicals such as fuel, acid, alkaline and saline solutions, and sewage, which greatly diminishes the structural life expectancy [5–10]. Essentially, acid penetration takes place primarily at the beginning of the diffusion process [11]. After the penetration of acid and water, hydrolysis of the polymer matrix occurs, followed by swelling. These are two common results of exposure to aggressive chemicals. Swelling leads to deformation of materials and causes early degradation [7,9,12–14]. During degradation, microdamage occurs and rapidly transforms into macroscopic cracks leading to sudden catastrophic failure. This microdamage is generally caused by stress concentration and the material's degradation [15–17].

Non-destructive techniques (NDT) are effective methods for addressing and mitigating structural health issues. Currently, there are many crack- and deformation-detection structural health monitoring (SHM) methods, such as those involving a material's electrical, acoustic, and optical properties [18–22]. Moreover, SHM approaches that detect chemical diffusion in composites are primarily based on changes in volume and weight measurements. However, these methods are impractical as they require disassembly of the structures [9,23]. Therefore, exploring different effects of the diffusion process might be beneficial.

In previous studies acid penetration was found to change the dielectric properties of the polymer nanocomposites. Measuring the conductivity and dielectric behavior of the polymer has been proven to be a good tool in monitoring chemical penetration processes [9,10,13,24,25]. Nevertheless, a certain percentage of nanofillers can increase the diffusion speed of the attacking chemicals due to agglomeration and pore formation. Furthermore, previous studies have shown that efficient dispersion of nano-additives affects the final physical properties of the nanocomposites [15,26–31]. For instance, Minelli et al. have suggested that the geometry and orientation of nano-additives affect the diffusion process [32]. Also, some studies have shown that two-dimensional materials, such as nano-clay, graphene, and boron nitride, are excellent barrier materials [32,33]. What is more, CNTs are known for their low electrical percolation thresholds, triggering conductive networks in a very efficient way and improving overall electrical properties. Moreover, the addition of CNTs also improves mechanical and thermal properties. The correct dispersion of CNTs, acting as reinforcements, benefits overall strength, stiffness, and durability. In addition, their high aspect ratio and the combination of outstanding mechanical, electrical and thermal properties positions them as ideal candidates for fabricating multifunctional composites [2,34–39].

For that reason, sensors using low concentrations of nano additives has been explored [9,40]. The conductive network is not properly established until the penetration of ions, which occurs during the early stages of the diffusion process. During the diffusion process, the attacking ions become the bridging units for this network. As a result, the conductivity of the nanocomposite increases upon penetration and can be used as an indicator for monitoring penetration. Thus, developing a monitoring system capable of detecting swelling and hydrolysis at an early stage of degradation would be a good approach, considering that swelling, corrosion, and hydrolysis are diffusion-limiting processes.

Nonetheless, it is essential to conduct extensive studies to understand and anticipate potential failures. It is necessary to employ characterization methods that can quantify the degradation that occurs over time during the diffusion process. These techniques can serve as benchmarks for potential NDT approaches, thereby facilitating effective structural health monitoring. The combination of DMA and nanoindentation is an effective technique as it provides valuable information, at nanoscale, that can be extrapolated to meso- and macroscales [4]. Moreover, the employment of contactless dielectric measurements with VNA could be complementary to the monitoring data in determining the big picture of the material's behavior at the different scales.

By combining two methods (mechanical and electrical characterization) this study employed a novel approach to studying the effects of acid diffusion on the physical properties of polymers containing different percentages of CNTs. The latter was performed through contactless monitoring of material changes after chemical attack using free-space measurements employing antennae in the microwave frequency range, while postprocess analysis involved DMA and nanoindentation to quantify these changes over time. By considering the relationship between CNT concentration, acid exposure, and mechanical properties, this study informs material selection and the development of damage-detection techniques in real-time. The integration of multiple measurement techniques, exemplified by the agreement between nanoindentation and VNA data, enables a comprehensive understanding of structural behavior, thereby enhancing the practices of wireless structural health monitoring.

## 2. Materials and Methods

### 2.1. Materials

Epoxy samples were prepared by incorporating various percentages of multi-wall CNTs into Epon 862 epoxy resin purchased from Hexion. The CNTs used in this study were purchased from Nanocyl and had dimensions ranging from 100 nm to 200 nm in diameter and 30 µm to 100 µm in length. The epoxy resin, specifically Epon 862, was thoroughly mixed with the appropriate amount of CNTs using a mechanical stirrer until a homogeneous mixture with low viscosity was obtained. Thereafter, a hardener, W32, was added. The resulting mixture was then poured into sheet molds with dimensions of 10 cm × 10 cm × 5 mm and cured at room temperature for 24 h.

### 2.2. Sample Preparation

To evaluate the effect of acid exposure on the epoxy/CNT composites, two sets of samples were subjected to acid exposure for different durations. One set of samples served as the control, while the other two sets were exposed to a testing acid solution with a concentration of 1 mol/L $H_2SO_4$. The acid exposure experiments were conducted for one week or one month. During the acid exposure period, the samples were immersed in the $H_2SO_4$ solution, allowing for interaction between the acidic environment and the epoxy/CNT composites. This acid exposure aimed to simulate the degradation effects that the composites may experience in real-world applications. Following the acid exposure, the samples underwent thorough rinsing with distilled water and drying at room temperature. Figure 1 shows the procedure to obtain the samples for mechanical testing. In Figure 1A, the samples exposed to acid were cut into rectangles, as depicted in B. The samples were then cut into smaller pieces in the x, y, and z dimensions using a diamond saw, resulting in each sample being divided into three equal zones for each CNT percentage. The samples were arranged so that Zone 1 was directly exposed to the acid with Zones 2 and 3 progressing from the skin to the core, as depicted in Figure 1C,D.

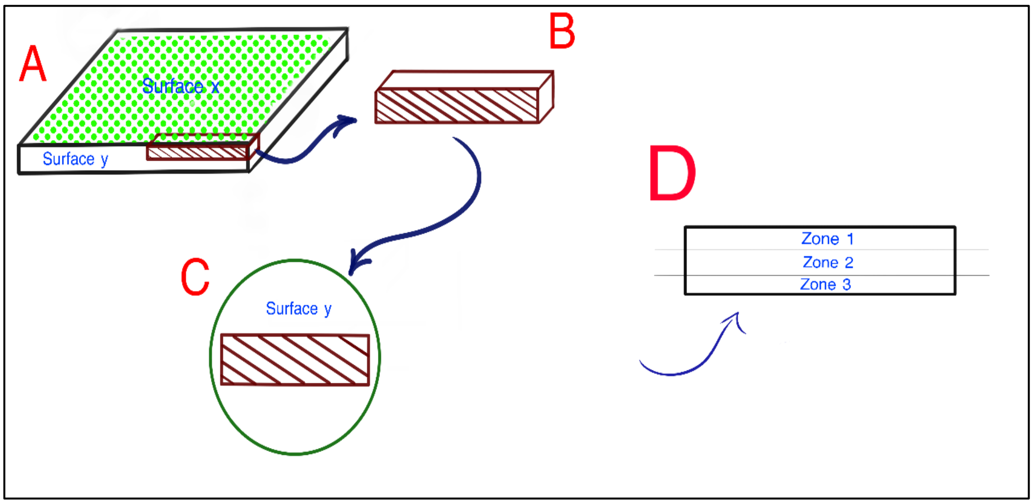


**Figure 1.** Illustration of sample preparation for mechanical testing. (**A**) Sample Surface exposed to acid. (**B**) Sample cut for mechanical testing. (**C**) Sample hold for nanoindentation. (**D**) Samples divided in Zones 1, 2 and 3.

### 2.3. Methods

All the tests and measurements were performed after the curing process of the epoxy/CNT composites was completed. It is important to note that the samples were not tested immediately after fabrication, but rather after the curing process, allowing the composites to fully develop their mechanical and chemical properties. First, the samples were characterized using the indentation testing technique, using a CSM Harness tester with a diamond indenter having an elastic modulus of 1141 GPa, Poisons' ratio of 0.07, and nominal angle of 136. The indentation parameters considered for the tests were: a maximum load of 1000 mN, a loading rate of 2000 mN/min, an unloading rate 2000 mN/min, and a pause of 15 s. In order to ensure reproducibility, each test was repeated many times. Twenty-one indents were made per sample, with 7 indents on each zone and a total of 63 indents per CNT percentage for a total of 378 indentations. The indentation measurements provided data on the local elastic modulus of the epoxy/CNT composites both before and after acid exposure. The influence of CNT percentage on the acid resistance of the composites was also evaluated in four steps:

1. Indenter pecks the surface;
2. Load phase up until the maximum load (1000 mN);
3. Hold the load;
4. Unload phase.

Additionally, the bulk mechanical properties of the samples were evaluated using 8000 PerkinElmer DMA equipment. The DMA experiments were conducted on the control samples, as well as on the samples before and after acid exposure. The samples were subjected to a sinusoidal stress at a frequency of 1 Hz using a three-point bending technique. A maximum stress of 50 MPa was applied at a constant room temperature of 25 °C. The DMA experiments generated stress–strain curves, allowing for an assessment of the impact of CNT percentage and acid exposure on the mechanical properties of the epoxy/CNT composites. The sample containing 5 wt% was investigated through a Keyence VHX 3D digital microscope.

At room temperature (25 °C), two 85131F flexible cables were connected to port 1 and port 2 for the measurements utilizing a VNA Agilent N230A 6000 (Figure 2). Calibration was performed using the E-Calibration Kit N4693-60003. Free-space measurements were conducted using two patch antennae with a central resonance frequency of 5 GHz. The diffraction effect at the edges of the samples was negligible due to the beamwidth of the antenna at the main lobe being three times smaller than the minimum transverse dimension of the samples [24]. The measurements were carried out in the far-field range within a frequency range of 3 GHz to 6 GHz. Initially, the return loss (S11) and insertion loss (S21) of the antenna were obtained in free space inside the anechoic chamber. Subsequently, the samples were positioned between the antennae at a distance of 25 mm, and a frequency sweep was triggered and the scattering parameters were measured through the Keysight Software and exported to Python.

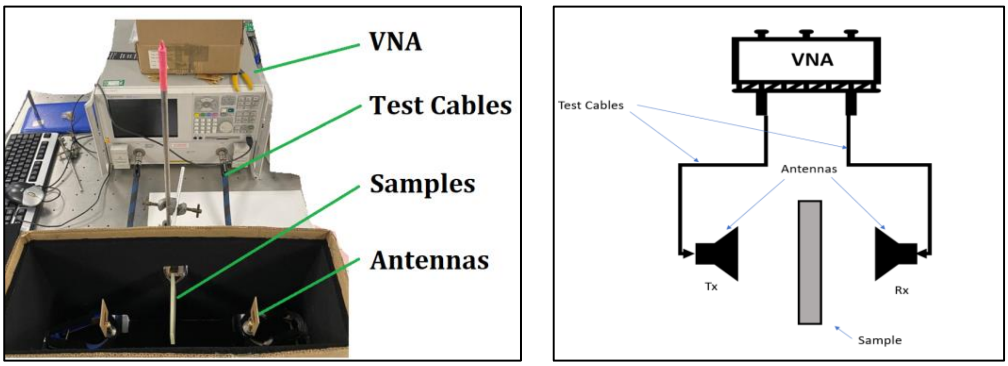


**Figure 2.** Experimental electromagnetic measurement set-up.

## 3. Results and Discussions

The control nanoindentations testing were performed on the 0, 2, and 5 wt% samples. This data were processed following the principal that in the three zones, the samples were homogeneous, thus showing that the sample remained constant across different zones before any acid exposure (Figure 3). The pristine sample's Young's modulus value of 7 GPa was greatly improved with the small addition of 2 wt%. At this percentage the mechanical properties had improved by almost 50%, reaching 12.5 GPA. Peculiarly, at 5 wt% the samples showed a minimal improvement of 1 GPa; moreover, in some cases even a detrimental effect could be spotted. This was because the agglomerates and agglomeration, along with the pores, reversed any benefit that the CNTs possessed. This would not be beneficial for applications where superior mechanical and electrical properties are expected [31,41–43].

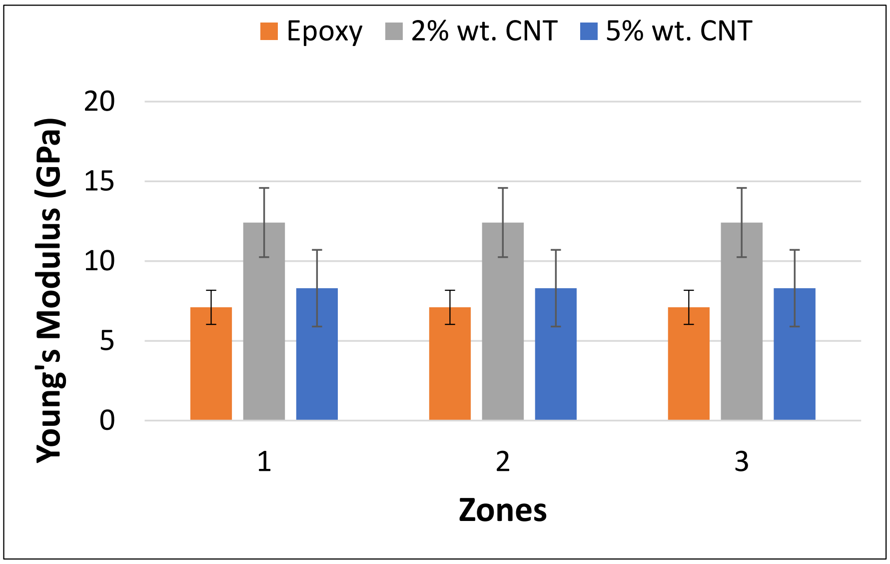


**Figure 3.** Elastic modulus of pristine epoxy and 2% wt. and 5% wt. CNT before acid attack.

Upon exposure to acid, notable changes in the mechanical behavior of the sample started to occur over time. As depicted in Figure 4, there was a distinct gradient in the mechanical properties of the sample, becoming more pronounced as the duration of acid exposure increased from one week to one month. The values in Zone 1, which was directly exposed to the acid solution, showed a noticeable deterioration compared to the control benchmark value. A 3 GPa reduction was present for both one week and one month of acid exposure. Notably, the impact in Zones 2 and 3 was almost negligible. This suggests that pristine samples have a lower percentage of porosity and thus fewer canals for acid diffusion. However, the gradient signifies that the sample's mechanical response was not uniform across its entirety but rather exhibited variations due to acid attack.

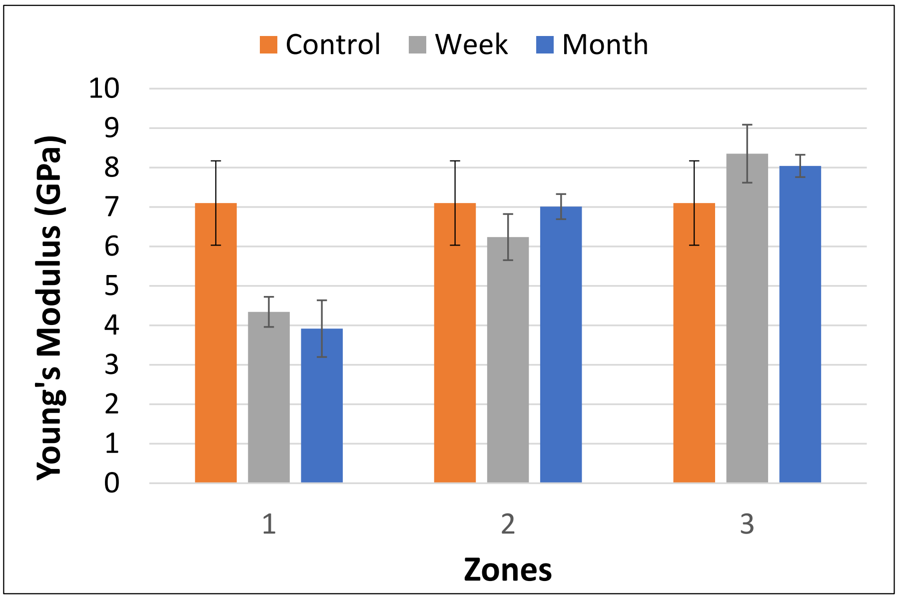


**Figure 4.** Elastic modulus of pristine epoxy before and after acid exposure.

Remarkably, the trend regarding acid exposure persisted even with small percentages of CNTs, such as 0.5 wt% and 1 wt%, as shown in the data presented in Figure 5. However, the samples behaved slightly differently. Although, the Young's modulus values after one month were around 2.5 GPa higher after one week, the 0.5 wt% samples depicted, throughout the three zones, the core-to-skin resistance effect. A possible reason could have been the morphology and the distribution in these areas [44,45]. On the other hand, at 1 wt%, more reasonable values after acid exposure were found. The Young's modulus was reduced by 2.5 GPa, principally in Zone 1, compared to one week of exposure, and therefore exhibited a visible change with increasing duration of acid exposure. This observation suggests that the presence of CNTs, even in relatively small numbers, influences the material's resistance to acid attack [16]. The reinforcing nature of the CNTs likely contributed to the improved acid resistance of the composite. The CNTs may act as barriers, hindering the penetration of acid and protecting the underlying polymer matrix.

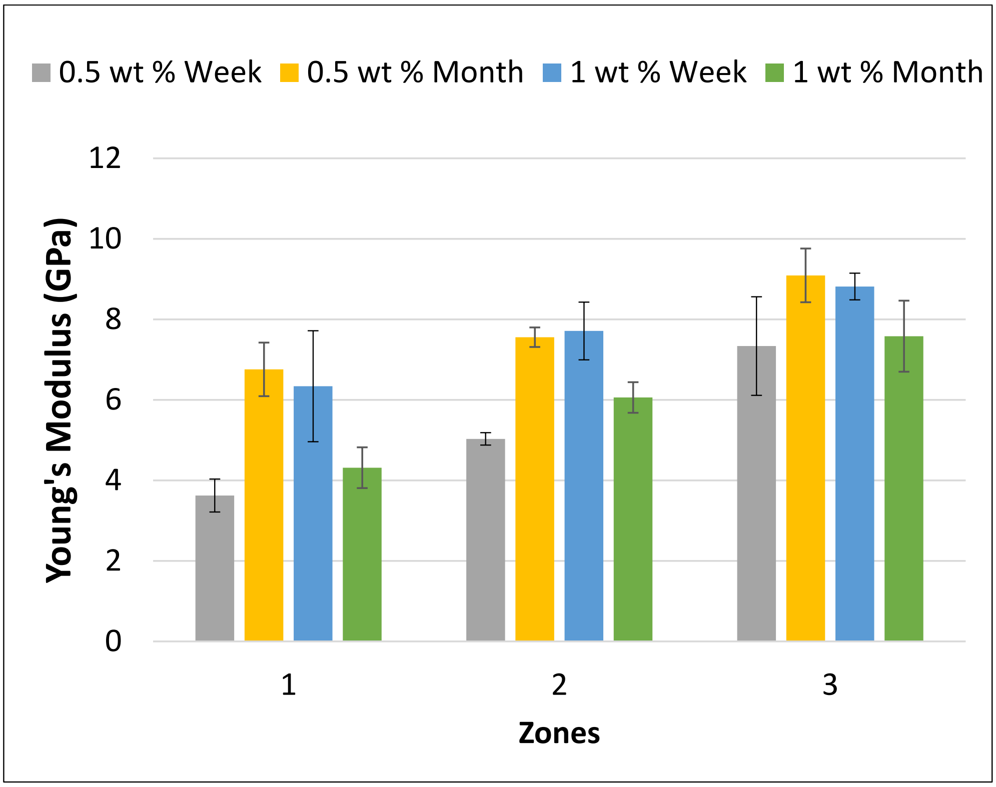


**Figure 5.** Elastic modulus of 0.5 wt% and 1 wt% after one week and month of acid exposure.

In Figure 6, for the sample containing 2 wt%, in Zones 1 and 2, after month of exposure, the Young's modulus went from 12.5 GPA to 7.4 GPA, a 40% decrease. A possible explanation is that the nanofillers started to debond, forming canals and allowing the penetration of the acid [46]. At Zone 3, the variation was just 1 GPa after month of exposure, indicating that the acid had not fully penetrated.

At a concentration of 4 wt% of CNTs, the material exhibited similar behavior to the sample containing 0.5 wt% and 2 wt% CNTs, as shown in Figure 7. The values for one month of exposure were greater than those for one week of exposure, especially in Zone 3. This could have been due, at the higher percentage, to the distribution, agglomerations and pores being problematic for the mechanical properties. However, the core-to-skin resistance effect was also present. This suggests that there is a critical threshold, known as the percolation threshold, at which the material's properties undergo a significant change [34,35,37,47]. Prior to reaching the percolation threshold, the reduction in mechanical properties can be primarily attributed to the presence of pores within the composite. These factors create weak points and discontinuities in the material, compromising its overall strength and stiffness.

Additionally, the pores and CNT agglomerates allow for increased acid penetration, further exacerbating the material's vulnerability to acid attack.

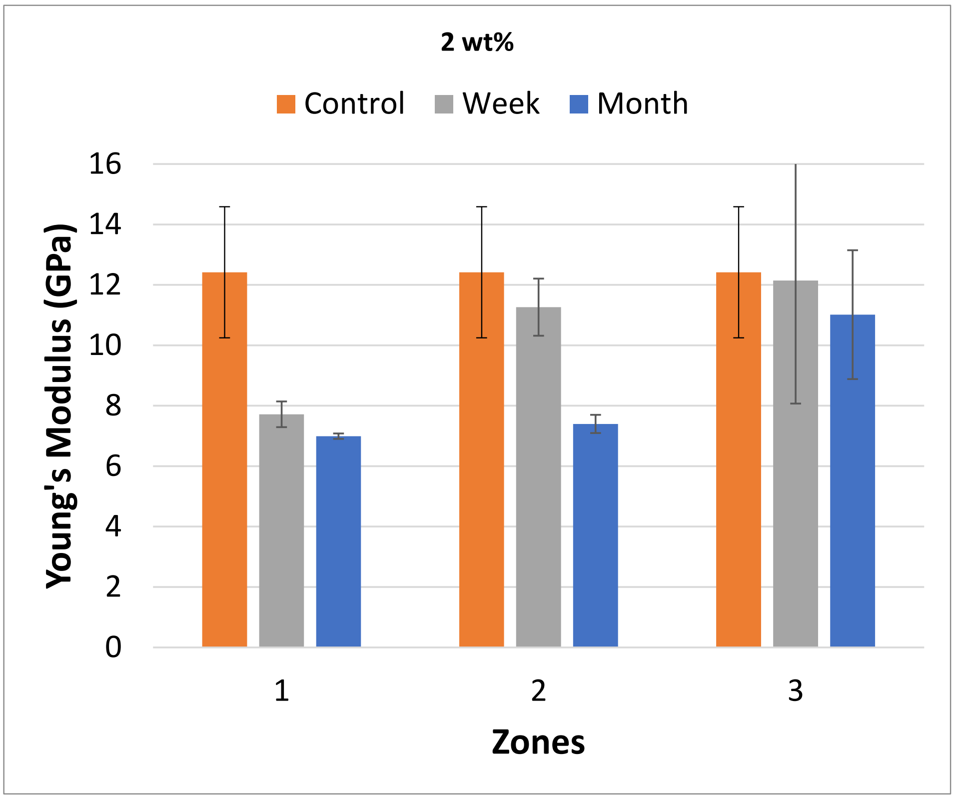


**Figure 6.** Elastic modulus of 2 wt% CNT sample before and after acid attack.

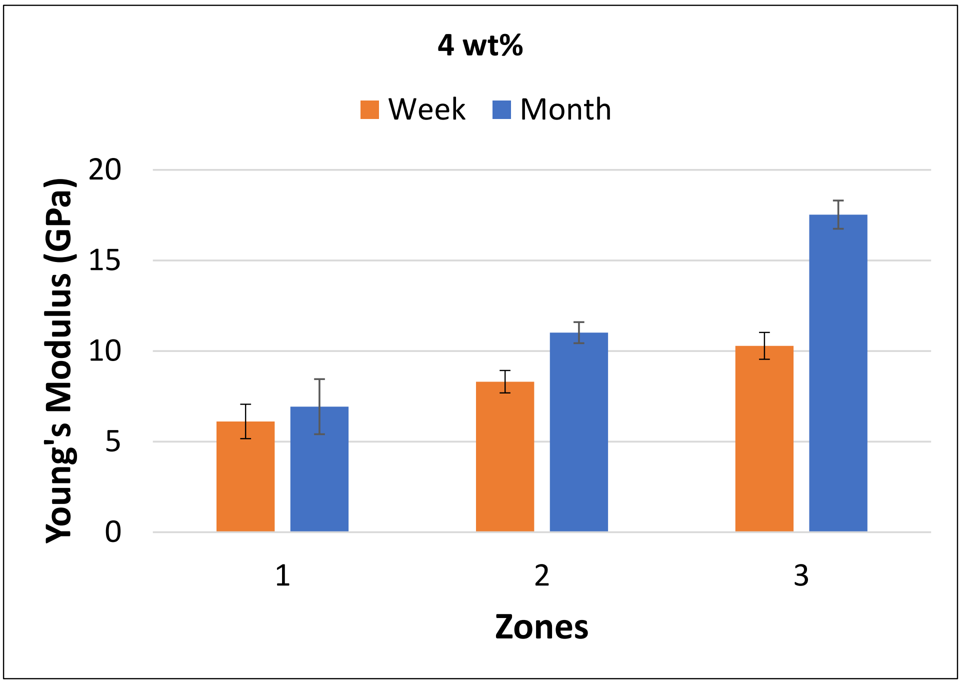


**Figure 7.** Elastic modulus of 4 wt% CNT sample before and after acid exposure.

Figure 8 shows that the detrimental effect for 5 wt% samples was more abrupt for Zones 1 and 2. Close to a 50% reduction in the Young's Modulus was found after as little as after one week and was maintained for month. This shows that at a concentration of

5 wt% of CNTs, agglomeration of the nanofillers becomes evident. This agglomeration leads to the formation of pores in the vicinity of the agglomerates, as depicted in Figure 9. Additionally, chemical reactions between the acid and polymer result in the formation of residues, indicated by the single arrows in Figure 10a. These residues exhibit varying shapes and dimensions, as shown in Figure 10b. Moreover, the formation of agglomerates and how the surroundings are affected is depicted with the green arrows [31,48].

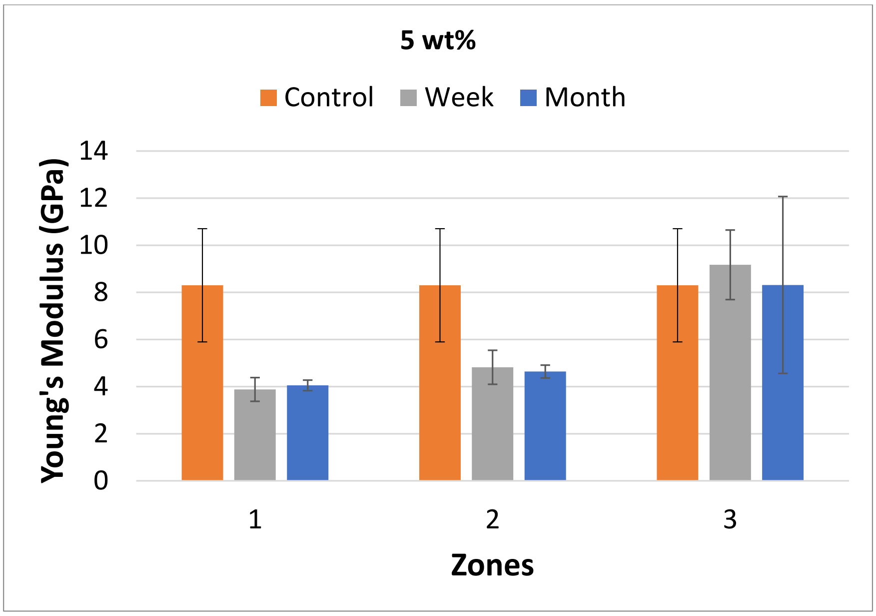


**Figure 8.** Elastic modulus of 5 wt% CNT sample before and after acid attack.

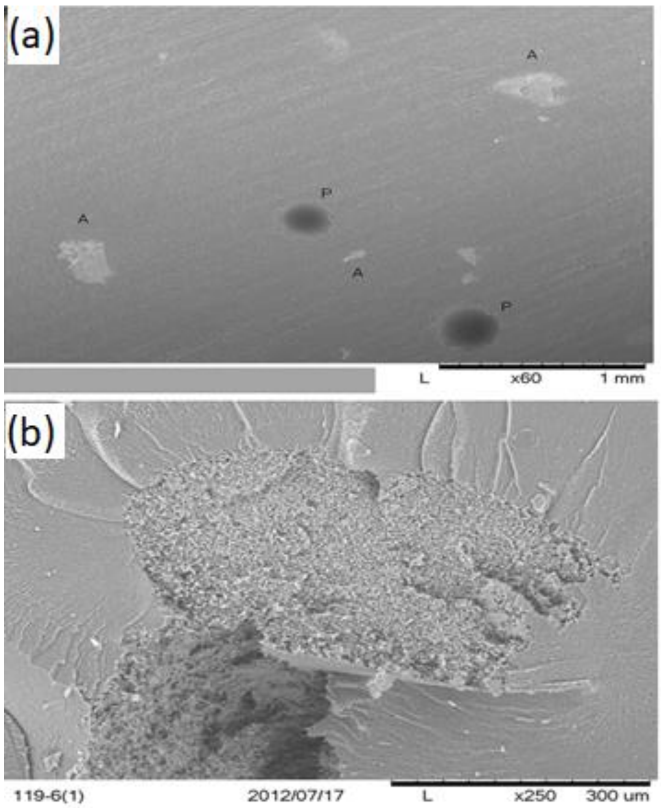


**Figure 9.** SEM characterization: (**a**) sample containing pores and agglomeration and (**b**) SEM ×250 image of agglomeration.

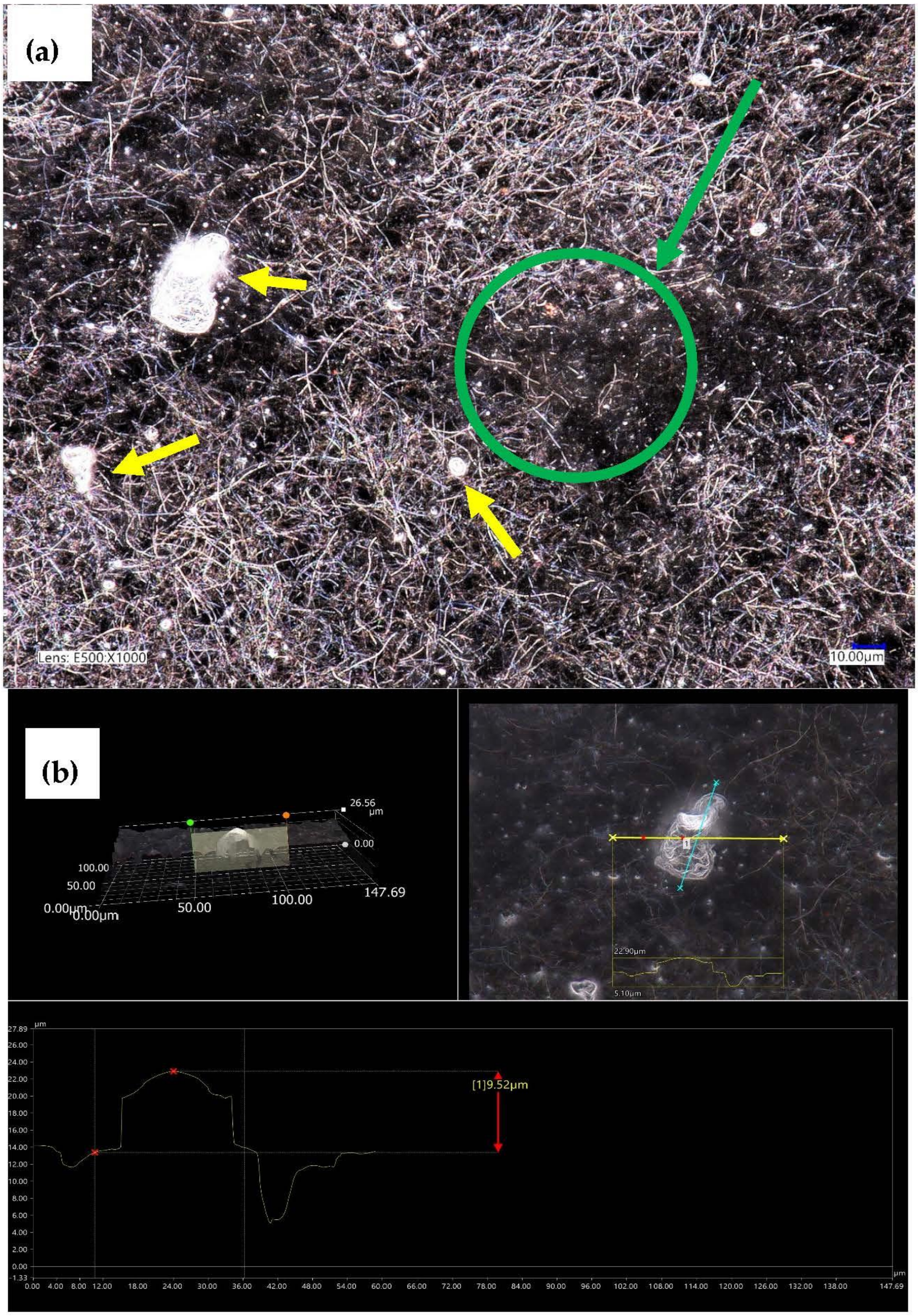


**Figure 10.** (**a**) 3D optical of 5 wt% CNT sample after one month of acid exposure and (**b**) pore dimension characterization through different perspectives.

It can be observed that both Zone 1 and Zone 2 exhibited similar reductions in the elastic modulus values. However, in Zone 3, the values of the elastic modulus appeared to be less affected. This can be attributed to the presence of CNT barriers, which impeded the acid diffusion and provided a protective effect. The barriers formed by the CNTs in this zone helped maintain the mechanical properties of the material, despite the acid exposure. This reduction indicates a decrease in the material's stiffness, which can be attributed to the accelerated diffusion of acid facilitated by the agglomerates and surrounding pores [11].

While CNTs generally act as a barrier against acid diffusion, the presence of agglomerates and the associated porous regions can have the unintended consequence of accelerating the diffusion of acid. The agglomerates, along with the porous surroundings, provide preferential paths for the acid to permeate into the composite material.

Figure 11 demonstrates the presence of a core-to-skin effect, indicating a gradient in mechanical properties from the core to the skin of the composite samples. This effect was observed independently of the percentage of CNTs present in the host polymer matrix. Regardless of the CNT concentration, the material's mechanical properties decreased as we moved closer to the surface that had been exposed to acid for a longer duration. The drop in mechanical properties was found to be proportional to the percentage of CNTs incorporated into the host polymer. This suggests that the presence of CNTs influences the material's resistance to acid attack, with higher concentrations providing better protection against mechanical degradation caused by acid exposure. It is worth mentioning that below 2 wt% the CNT produced a slight improvement in the mechanical properties. Moreover, at 0.5 wt% and 1 wt% the reduction of the Young's modulus started to be more noticeable evenly through the zones. This was due to that acid profiting from the smaller barrier, and instead exploiting the weak bonds as canals for diffusion. Above the percolation threshold (i.e., 2, 4, and 5 wt%) the behavior was similar.

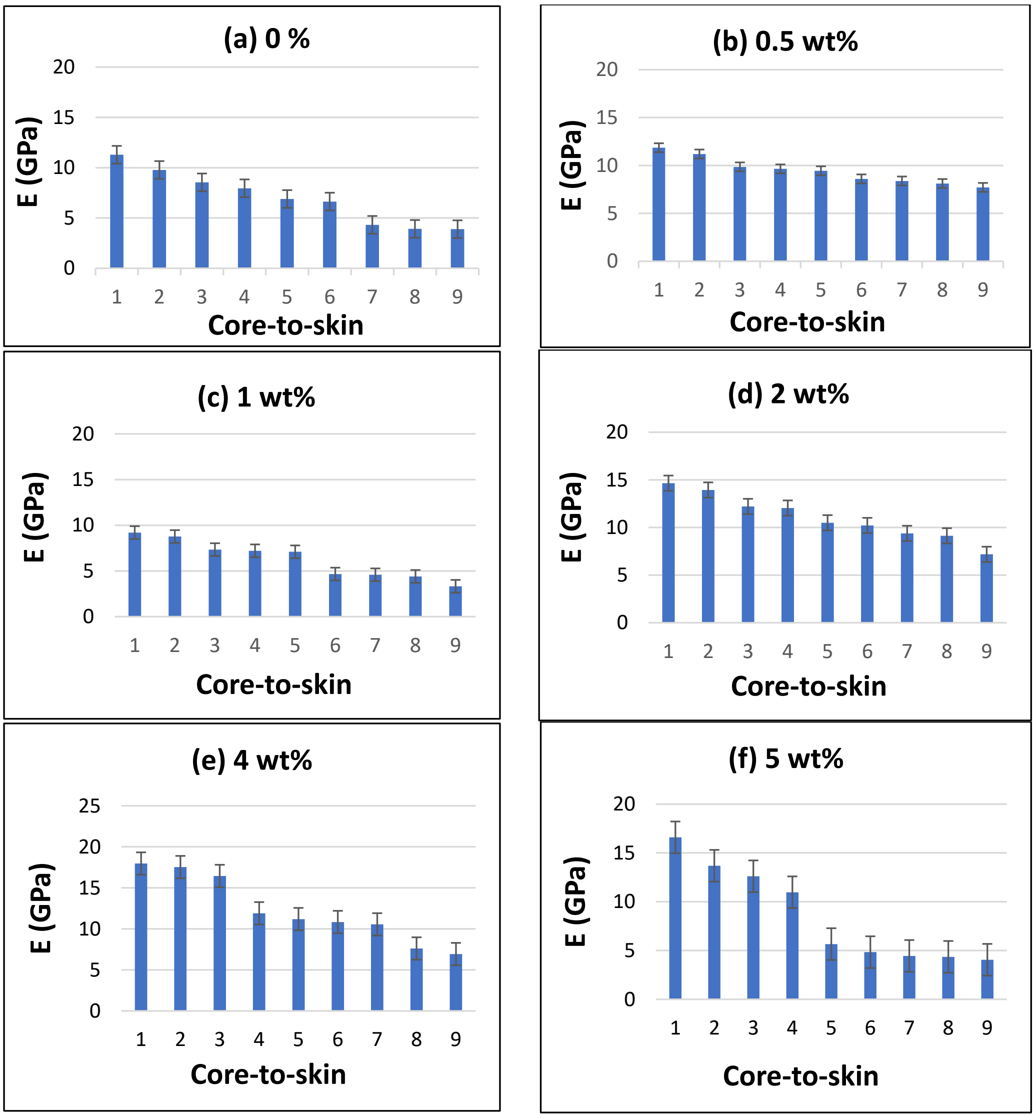


**Figure 11.** Nanoindentation zones (core-to-skin) of Young's modulus data after one month of acid exposure.

The mechanical data obtained using DMA, are depicted in Figure 12. The DMA shows the bulk mechanical properties. The same behavior as at nanoscale is shown for the control values. The optimal mechanical enhancements reached a peak at 2 wt% and, surprisingly, at one week of exposure, and specifically at 2 wt%, the Young's modulus seemed to have improved. At 2 wt% the Young's modulus showed an augmentation of 3 GPA compared to control, that was reduced by 3 GPA after one month of exposure. The reverse was expected.

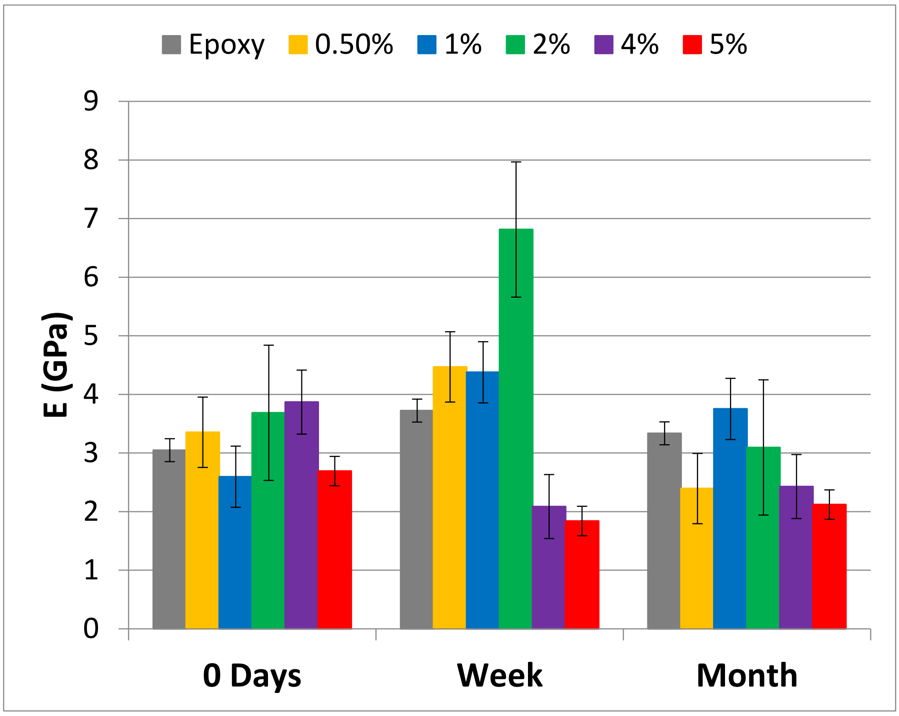


**Figure 12.** DMA of Young's modulus bulk data for control, week, and month samples.

Figures 13 and 14 clearly demonstrate that the percentage of CNTs incorporated into the composite material had a significant impact on the return loss parameter. The trend was progressive, meaning that as the CNT concentration approached the percolation threshold, there was a noticeable alteration in the return loss [49,50].

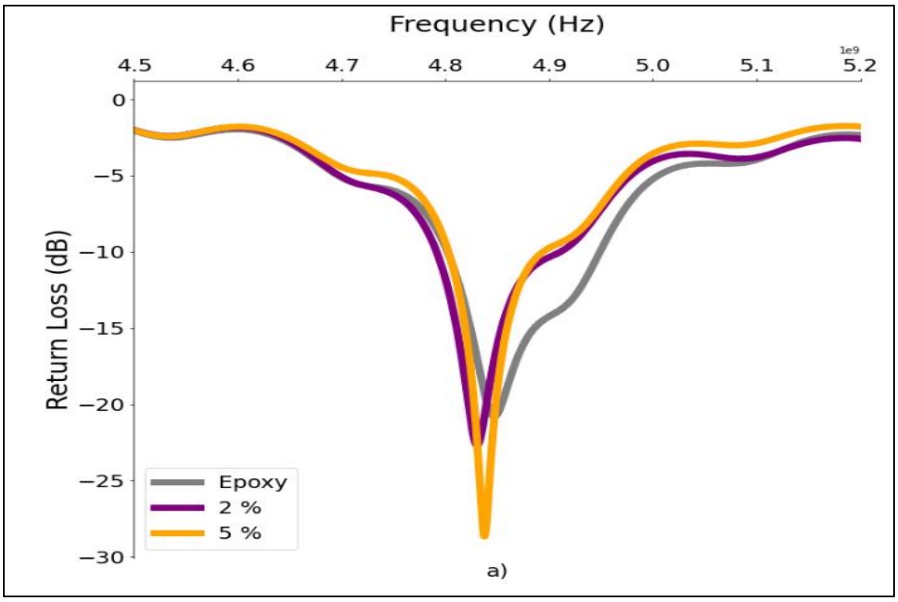


**Figure 13.** VNA scattering (S11) results before acid exposure.

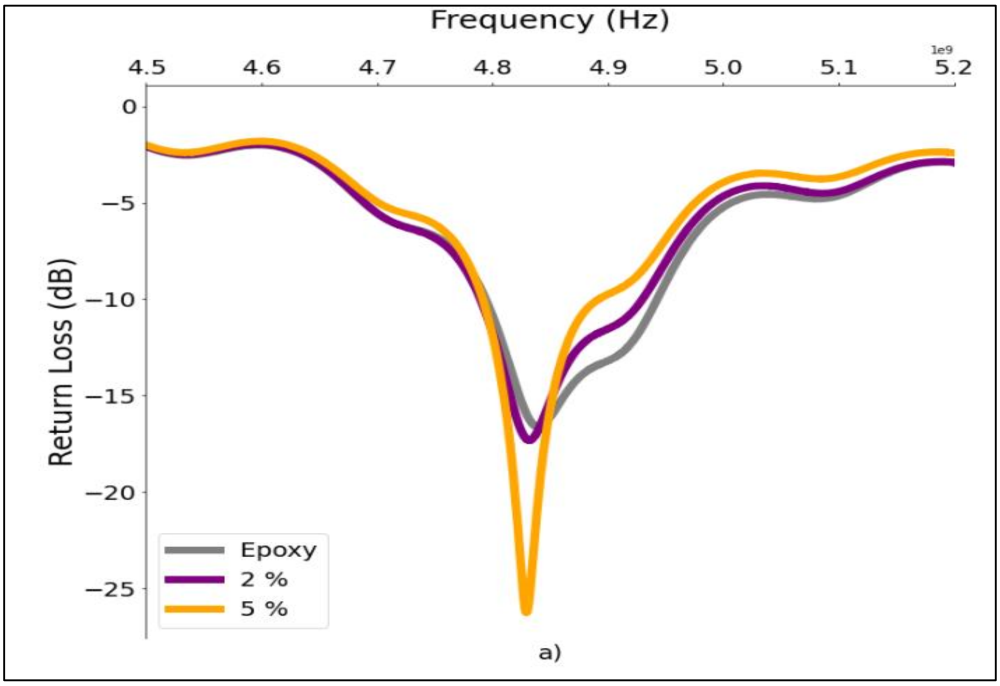


**Figure 14.** VNA scattering (S11) results after one month of acid exposure.

Upon exposure to acid attack, the characteristics of the material undergo changes as a result of ion diffusion. This diffusion process directly affects the dielectric properties of the material, including its permittivity and permeability. These changes in dielectric properties are reflected in the measurements obtained through free space using a patch antenna [51–54].

By introducing CNT fillers into the composite, the material becomes more conductive, primarily due to the formation of a conductive network facilitated by the presence of CNTs. This conductive network significantly alters the dielectric properties of the material. Consequently, the change in attenuation observed in the measurements is directly dependent on the concentration of CNTs present in the composite.

As the concentration of CNTs increases, the return loss decreases. This decrease is an indication of improved conductivity and altered dielectric properties of the composite material. The change in attenuation, reflected in the return loss measurements, serves as a reliable indicator of the influence of CNT concentration on the material's electromagnetic characteristics.

The results obtained from the free-space technique, specifically the S-parameter (S11) values, are illustrated in Figure 15. As the percentage of CNTs increased in the control samples, the absolute values of the S11 parameter also exhibited an increase, as anticipated. This correlation indicates that higher CNT concentrations contribute to improved electromagnetic characteristics.

However, a significant observation was made when the CNT percentage reached the electrical percolation threshold, which occurred at approximately 2%. At this threshold, the CNTs started to act as a barrier to the diffusion process. This behavior was clear in the 2% CNT sample. In contrast, the pristine epoxy material experienced acid diffusion after just one week, and this trend continued after one month. These findings suggest that the diffusion was not impeded, and the alteration in the dielectric properties remained consistent.

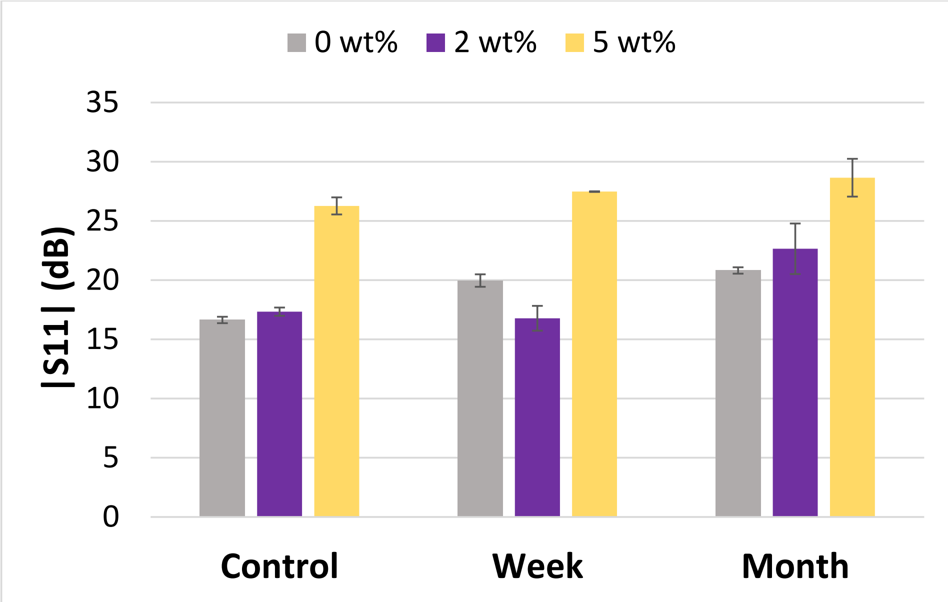


**Figure 15.** VNA absolute scattering (S11) results comparison before and after acid exposure.

In the case of the 5% CNT sample, a slight gradual increase in the difference between the control sample, the one-week exposure, and the one-month exposure was observed. This can be attributed to the fact that the dielectric properties had already been affected by the percentage of CNTs, reaching a plateau. This behavior aligns with the principle of the electrical percolation threshold, where the properties of the composite material experience significant changes as the CNT concentration surpasses a certain threshold.

It is worth noting that at higher CNT percentages, the barrier effect provided by the CNTs becomes more pronounced. However, it is important to consider that the formation of CNT aggregates can inadvertently facilitate diffusion by triggering the creation of pores in their surrounding regions. These pores serve as channels for ions to diffuse, counteracting the barrier effect to some extent.

Our findings indicate that as the amount of CNTs in the host matrix increases and the material is exposed to acid for extended periods, a net reduction in the mechanical properties is observed. This phenomenon aligns with our previous studies, where we also observed the adverse effects of CNT agglomerates and agglomeration on the material properties. When the exposure time to acid was relatively short, the reinforcing properties of the CNTs were predominant, leading to improvements in the mechanical performance of the composite. This is consistent with the initial trend we observed, where the addition of CNTs, even in small percentages, enhanced the material's properties.

However, with prolonged exposure to acid, the agglomeration of CNTs becomes more pronounced, negatively impacting the material's mechanical properties. The formation of CNT agglomerates creates regions of weak bonding and reduced load transfer within the composite. These agglomerates act as stress concentrators and sites for potential crack initiation, ultimately leading to a reduction in the material's overall strength and stiffness.

The presence of CNT agglomerates also hinders the effective dispersion of CNTs within the matrix, limiting their ability to reinforce the composite structure. As a result, the benefits provided by the CNTs are outweighed by the detrimental effects of agglomeration, leading to a decline in mechanical properties over prolonged exposure to acid.

During the acid-exposure experiments, the diffusion of ions resulted in alterations in the physical properties of the epoxy/CNT composites. Furthermore, it was found that the percentage of CNTs added to the polymer influenced these properties. These insights emphasize the importance of considering both the mechanical and electromagnetic properties in SHM applications. By understanding the behavior of materials under different conditions, such as the presence of CNTs and exposure to acid, this knowledge can be utilized in the development of robust SHM strategies. The observed sensitivity of the mechanical properties to the amount of CNTs, and the identification of degradation patterns, can guide the selection and optimization of materials for SHM applications.

## 4. Conclusions

In this study, we fabricated various samples with increasing amounts of CNT, ranging from 0% to 5%. To assess their mechanical properties, we employed two different techniques: bulk mechanical properties were measured using DMA, while local mechanical properties were evaluated using nanoindentation. Our findings clearly demonstrate that the mechanical properties of the samples were highly sensitive to both the presence of agglomerations and the percentage of CNT added to the polymer. Notably, we observed a distinct dependence of the material's behavior on the carbon fillers before, during, and after the percolation threshold.

Subsequently, we subjected the samples to acid exposure and monitored the changes in their mechanical properties over time. Our observations revealed that the material began to degrade progressively as the duration of acid exposure increased, ranging from one week to one month. However, the extent of degradation was found to be dependent on the amount of CNT present in the host polymer. We observed degradation occurring at both nanoscale and macroscale. At macroscale, the increase in CNT percentage led to a more pronounced reduction in mechanical properties, primarily due to the presence of larger aggregates and increased porosity. At nanoscale, all samples exhibited a consistent behavior, demonstrating a visible gradient in mechanical properties from the core to the skin region, which comes into contact with the acid solution. Notably, this gradient became more prominent as the amount of CNT in the host polymer increased.

An agreement was observed between the data obtained from the nanoindentation technique (mechanical) and VNA measurements (electromagnetic). This agreement signifies the potential for employing multi-modal sensing approaches in structural health monitoring (SHM) and highlights the relevance of the study to wireless SHM applications. Additionally, the observed gradient in mechanical properties at nanoscale presents an opportunity for real-time damage detection and assessment in SHM systems. Integrating multiple measurement techniques, as demonstrated by the agreement between nanoindentation and VNA data, can provide a comprehensive understanding of structural behavior and facilitate more effective SHM practices in wireless applications.

**Author Contributions:** Conceptualization, K.L.; methodology, K.L. and M.T.; validation, K.L. and M.T.; formal analysis, S.T.-V.; investigation, M.D. and K.K.L.; writing—original draft preparation, S.T.-V.; writing—review and editing, S.T.-V. and K.L.; supervision, K.L.; project administration, K.L. All authors have read and agreed to the published version of the manuscript.

**Funding:** This research received no external funding.

**Data Availability Statement:** Not applicable.

**Conflicts of Interest:** The authors declare no conflict of interest.

## References

1. Goyal, R.K. *Nanomaterials and Nanocomposites: Synthesis, Properties, Characterization Techniques, and Applications*; CRC Press: Boca Raton, FL, USA, 2017; ISBN 9781498761673.
2. Loos, M. *Carbon Nanotube Reinforced Composites*, 1st ed.; William Andrew: Oxford, UK, 2015; Volume 3, ISBN 9781455778980.
3. Kar, K.; Pandey, J.; Rana, S. (Eds.) *Handbook of Polymer Nanocomposites. Processing, Performance and Application Volume B Carbon Nanotube Based Polymer Composites*; Springer: Berlin/Heidelberg, Germany, 2015.
4. Ren, X.; Burton, J.; Seidel, G.D.; Lafdi, K. Computational Multiscale Modeling and Characterization of Piezoresistivity in Fuzzy Fiber Reinforced Polymer Composites. *Int. J. Solids Struct.* **2015**, *54*, 121–134. [CrossRef]
5. Tanks, J.D.; Arao, Y.; Kubouchi, M. Diffusion Kinetics, Swelling, and Degradation of Corrosion-Resistant C-Glass/Epoxy Woven Composites in Harsh Environments. *Compos. Struct.* **2018**, *202*, 686–694. [CrossRef]
6. Gotou, T.; Noda, M.; Tomiyama, T.; Sembokuya, H.; Kubouchi, M.; Tsuda, K. In Situ Health Monitoring of Corrosion Resistant Polymers Exposed to Alkaline Solutions Using PH Indicators. *Sens. Actuators B Chem.* **2006**, *119*, 27–32. [CrossRef]

7. Liu, C.; Lafdi, K. Environmental Monitoring of Composite Durability Use Multiple Sensing Technologies. In Proceedings of the Composites and Advanced Materials Expo, Dallas, TX, USA, 18 October 2018.
8. Liu, Y.; Kubouchi, M.; Sembokuya, H.; Tsuda, K.; Tomiyama, T. On-Line Monitoring of Epoxy Resin Exposed to Acid Solution. *J. Mater. Sci. Technol.* **2006**, *22*, 414–418.
9. Liu, C.; Sergeichev, I.; Akhatov, I.; Lafdi, K. CNT and Polyaniline Based Sensors for the Detection of Acid Penetration in Polymer Composite. *Compos. Sci. Technol.* **2018**, *159*, 111–118. [CrossRef]
10. Liu, C.; Lafdi, K.; Chinesta, F. Durability Sensor Using Low Concentration Carbon Nano Additives. *Compos. Sci. Technol.* **2020**, *195*, 108200. [CrossRef]
11. Crank, J. *The Mathematics of Diffusion*; Oxford Science Publications: Oxford, UK, 1975.
12. Abastari; Sakai, T.; Sembokuya, H.; Kubouchi, M.; Tsuda, K. Study on Permeation Behavior and Chemical Degradation of PA66 in Acid Solution. *Polym. Degrad. Stab.* **2007**, *92*, 379–388. [CrossRef]
13. La Saponara, V. Environmental and Chemical Degradation of Carbon/Epoxy and Structural Adhesive for Aerospace Applications: Fickian and Anomalous Diffusion, Arrhenius Kinetics. *Compos. Struct.* **2011**, *93*, 2180–2195. [CrossRef]
14. Starkova, O.; Buschhorn, S.T.; Mannov, E.; Schulte, K.; Aniskevich, A. Water Transport in Epoxy/MWCNT Composites. *Eur. Polym. J.* **2013**, *49*, 2138–2148. [CrossRef]
15. Benyahia, H.; Tarfaoui, M.; Datsyuk, V.; El Moumen, A.; Trotsenko, S.; Reich, S. Dynamic Properties of Hybrid Composite Structures Based Multiwalled Carbon Nanotubes. *Compos. Sci. Technol.* **2017**, *148*, 70–79. [CrossRef]
16. Tarfaoui, M.; Lafdi, K.; El Moumen, A. Mechanical Properties of Carbon Nanotubes Based Polymer Composites. *Compos. Part B Eng.* **2016**, *103*, 113–121. [CrossRef]
17. Beaumont, P.W.R.; Soutis, C. Structural Integrity of Engineering Composite Materials: A Cracking Good Yarn. *Philos. Trans. R. Soc. A* **2016**, *374*, 1–7. [CrossRef] [PubMed]
18. Shull, P.J. *Nondestrutive Evaluation Theory, Techniques and Applications*; Marcel Dekker Inc.: New York, NY, USA, 2002; ISBN 0824788729.
19. Balageas, D.; Fritzen, C.-P.; Güemes, A. *Structural Health Monitoring*; ISTE: Londond, UK, 2006; ISBN 9780470741337.
20. Güemes, A.; Fernandez-Lopez, A.; Pozo, A.R.; Sierra-Peréz, J. Structural Health Monitoring for Advanced Composite Structures: A Review. *J. Compos. Sci.* **2020**, *4*, 13. [CrossRef]
21. Raju, R. Structural Health Monitoring of Composites for Aircraft Structures. In Proceedings of the International Conference on Advancements and Futuristic Trends in Mechanical and Materials Engineering, Kapurthala, India, 16–18 October 2014.
22. Boller, C.; Chang, F.-K.; Fujino, Y. *Encyclopedia of Structural Health Monitoring*; Wiley: Hoboken, NJ, USA, 2009; ISBN 9780470058220.
23. Tamayo-Vegas, S.; Lafdi, K. A Literature Review of Non-Contact Tools and Methods in Structural Health Monitoring. *Eng. Technol. Open Access J.* **2021**, *4*, 555626. [CrossRef]
24. Tamayo-Vegas, S.; Lafdi, K.; Elsdon, M. A Contactless Characterization of CNT/Epoxy Nanocomposites Behavior under Acid Exposure. *Compos. Struct.* **2023**, *305*, 116508. [CrossRef]
25. Al Habis, N.; Liu, C.; Dumuids, J.B.; Lafdi, K. Intelligent Design of Conducting Network in Polymers Using Numerical and Experimental Approaches. *RSC Adv.* **2016**, *6*, 95010–95020. [CrossRef]
26. Tjong, S.C. *Electrical and Dielectric Behavior of Carbon Nanotube-Filled Polymer Composites*; Woodhead Publishing Limited: Sawston, UK, 2010; ISBN 9781845696726.
27. Bauhofer, W.; Kovacs, J.Z. A Review and Analysis of Electrical Percolation in Carbon Nanotube Polymer Composites. *Compos. Sci. Technol.* **2009**, *69*, 1486–1498. [CrossRef]
28. Kovacs, J.Z.; Velagala, B.S.; Schulte, K.; Bauhofer, W. Two Percolation Thresholds in Carbon Nanotube Epoxy Composites. *Compos. Sci. Technol.* **2007**, *67*, 922–928. [CrossRef]
29. Sandler, J.; Shaffer, M.S.P.; Prasse, T.; Bauhofer, W.; Schulte, K.; Windle, A.H. Development of a Dispersion Process for Carbon Nanotubes in an Epoxy Matrix and the Resulting Electrical Properties. *Polymer* **1999**, *40*, 5967–5971. [CrossRef]
30. Khammassi, S.; Tarfaoui, M.; Lafdi, K. Study of Mechanical Performance of Polymer Nanocomposites Reinforced with Exfoliated Graphite of Different Mesh Sizes Using Micro-Indentation. *J. Compos. Mater.* **2021**, *55*, 2617–2629. [CrossRef]
31. Tamayo-Vegas, S.; Muhsan, A.; Liu, C.; Tarfaoui, M.; Lafdi, K. The Effect of Agglomeration on the Electrical and Mechanical Properties of Polymer Matrix Nanocomposites Reinforced with Carbon Nanotubes. *Polymers* **2022**, *14*, 1842. [CrossRef] [PubMed]
32. Minelli, M.; Baschetti, M.G.; Doghieri, F. Analysis of Modeling Results for Barrier Properties in Ordered Nanocomposite Systems. *J. Membr. Sci.* **2009**, *327*, 208–215. [CrossRef]
33. Gomasang, P.; Kawahara, K.; Yasuraoka, K.; Maruyama, M.; Ago, H.; Okada, S.; Ueno, K. A Novel Graphene Barrier against Moisture by Multiple Stacking Large-Grain Graphene. *Sci. Rep.* **2019**, *9*, 3777. [CrossRef] [PubMed]
34. Kirkpatrick, S. Percolation and Conduction. *Rev. Mod. Phys.* **1973**, *45*, 574–588. [CrossRef]
35. Stauffer, D.; Aharony, A. *Introduction to Percolation Theory*; Taylor & Francis: London, UK, 1994.
36. Du, F.; Scogna, R.C.; Zhou, W.; Brand, S.; Fischer, J.E.; Winey, K.I. Nanotube Networks in Polymer Nanocomposites: Rheology and Electrical Conductivity. *Macromolecules* **2004**, *37*, 9048–9055. [CrossRef]
37. Hu, N.; Masuda, Z.; Yan, C.; Yamamoto, G.; Fukunaga, H.; Hashida, T. The Electrical Properties of Polymer Nanocomposites with Carbon Nanotube Fillers. *Nanotechnology* **2008**, *19*, 21. [CrossRef]

38. Duong, H.M.; Tran, T.Q.; Kopp, R.; Myint, S.M.; Peng, L. Direct Spinning of Horizontally Aligned Carbon Nanotube Fibers and Films from the Floating Catalyst Method. In *Nanotube Superfiber Materials: Science, Manufacturing, Commercialization*; Elsevier: Amsterdam, The Netherlands, 2019; pp. 3–29. ISBN 9780128126677.
39. Duong, H.M.; Myint, S.M.; Tran, T.Q.; Le, D.K. Post-Spinning Treatments to Carbon Nanotube Fibers. In *Carbon Nanotube Fibres and Yarns: Production, Properties and Applications in Smart Textiles*; Elsevier: Amsterdam, The Netherlands, 2019; pp. 103–134. ISBN 9780081027226.
40. Tarfaoui, M.; El Moumen, A.; Lafdi, K. Progressive Damage Modeling in Carbon Fibers/Carbon Nanotubes Reinforced Polymer Composites. *Compos. Part B Eng.* **2017**, *112*, 185–195. [CrossRef]
41. Maghsoudlou, M.A.; Barbaz Isfahani, R.; Saber-Samandari, S.; Sadighi, M. Effect of Interphase, Curvature and Agglomeration of SWCNTs on Mechanical Properties of Polymer-Based Nanocomposites: Experimental and Numerical Investigations. *Compos. Part B Eng.* **2019**, *175*, 107119. [CrossRef]
42. Zare, Y. Study of Nanoparticles Aggregation/Agglomeration in Polymer Particulate Nanocomposites by Mechanical Properties. *Compos. Part A Appl. Sci. Manuf.* **2016**, *84*, 158–164. [CrossRef]
43. Tamayo-Vegas, S.; Muhsan, A.; Chang, L.; Tarfaoui, M.; Lafdi, K. Effect of CNT Additives on the Electrical Properties of Derived Nanocomposites (Experimentally and Numerical Investigation). *Mater. Today Proc.* **2021**, *52*, 199–205. [CrossRef]
44. Monticeli, F.M.; Montoro, S.R.; Voorwald, H.J.C.; Cioffi, M.O.H. Porosity Characterization of Carbon Fiber/Epoxy Composite Using Hg Porosimetry and Other Techniques. *Polym. Eng. Sci.* **2020**, *60*, 841–849. [CrossRef]
45. Fang, Q.; Lafdi, K. Effect of Nanofiller Morphology on the Electrical Conductivity of Polymer Nanocomposites. *Nano Express* **2021**, *2*, 010019. [CrossRef]
46. Govorov, A.; Wentzel, D.; Miller, S.; Kanaan, A.; Sevostianov, I. Electrical Conductivity of Epoxy-Graphene and Epoxy-Carbon Nanofibers Composites Subjected to Compressive Loading. *Int. J. Eng. Sci.* **2018**, *123*, 174–180. [CrossRef]
47. Sahimi, M. *Applications of Percolation Theory*; Taylor & Francis: London, UK, 1995.
48. Machrafi, H.; Lebon, G.; Iorio, C.S. Effect of Volume-Fraction Dependent Agglomeration of Nanoparticles on the Thermal Conductivity of Nanocomposites: Applications to Epoxy Resins, Filled by $SiO_2$, AlN and MgO Nanoparticles. *Compos. Sci. Technol.* **2016**, *130*, 78–87. [CrossRef]
49. Wee, F.H.; Soh, P.J.; Suhaizal, A.H.M.; Nornikman, H.; Ezanuddin, A.A.M. Free Space Measurement Technique on Dielectric Properties of Agricultural Residues at Microwave Frequencies. In Proceedings of the 2009 SBMO/IEEE MTT-S International Microwave and Optoelectronics Conference (IMOC), Belem, Brazil, 3–6 November 2009; pp. 183–187. [CrossRef]
50. Katsounaros, A.; Rajab, K.Z.; Hao, Y.; Mann, M.; Milne, W.I. Microwave Characterization of Vertically Aligned Multiwalled Carbon Nanotube Arrays. *Appl. Phys. Lett.* **2011**, *98*, 203105. [CrossRef]
51. Xin, H.; Wang, L.; Carnahan, D. Characterization of Multi-Walled Carbon Nanotube (MWNT) Papers Using X-Band Waveguides. In Proceedings of the IEEE MTT-S International Microwave Symposium Digest, Honolulu, HI, USA, 3–8 June 2007; pp. 1181–1184. [CrossRef]
52. Afsar, M.N.; Afsar, M.N.; Birch, J.R.; Clarke, R.N.; Chantry, G.W. The Measurement of the Properties of Materials. *Proc. IEEE* **1986**, *74*, 183–199. [CrossRef]
53. Ghodgaonkar, D.K.; Varadan, V.V.; Varadan, V.K. A Free-Space Method for Measurement of Dielectric Constants and Loss Tangents at Microwave Frequencies. *IEEE Trans. Instrum. Meas.* **1989**, *38*, 789–793. [CrossRef]
54. Wiesbeck, W.; Kahny, D. Single Reference, Three Target Calibration and Error Correction For Monostatic, Polarimetric Free Space Measurements. *Proc. IEEE* **1991**, *79*, 1551–1558. [CrossRef]